

Top-forms of Leading Singularities in Nonplanar Multi-loop Amplitudes

Baoyi Chen,¹ Gang Chen,^{1,*} Yeuk-Kwan E. Cheung,^{1,†} Ruofei Xie,¹ and Yuan Xin¹

¹*Department of Physics, Nanjing University, 22 Hankou Road, Nanjing 210098, China*

Bipartite on-shell diagram is the latest tool in constructing scattering amplitudes. In this letter we prove that an on-shell diagram process a rational top-form if and only if the algebraic ideal comprised of the geometrical constraints can be shifted linearly during successive Britto-Cachazo-Feng-Witten (BCFW) integrations. With a proper geometric interpretation of the constraints in the Grassmannian manifold, the top-form integration contours can thus be obtained, and understood, in a straightforward way. All top-form integrands can be obtained with the BCFW bridge decomposition chain. For on-shell diagrams without external BCFW-bridges, an extra step of adding an auxiliary external momentum line and the taking the soft limit is needed. This completes the top-form description of leading singularities in nonplanar scattering amplitudes of $\mathcal{N} = 4$ Super Yang-Mills (SYM), which is valid for arbitrary higher-loops and beyond the Maximally-Helicity-Violation (MHV) amplitudes.

Introduction Bipartite diagrams and the associated Grassmannian geometry [1, 2] have recently found their way into the scattering amplitudes studies. An amazing discovery was to exploit them in computing scattering amplitudes in $\mathcal{N} = 4$ SYM theory [3–10]. Planar scattering amplitudes are represented by on-shell bipartite diagrams and expressed in “top-form” as contour integrations over the Grassmannian submanifolds. Planar loop integrands in $\mathcal{N} = 4$ SYM have recently been constructed in [3, 11] along with the introduction of the Grassmannian and on-shell method. As a result, the “dlog” form and the Yangian symmetry [12–16] of the scattering amplitudes are made manifest in the planar limit. It is natural to extend the construction to non-planar scattering amplitudes [17, 18, 20–22], and theories of reduced (super) symmetries [23–25].

The leading singularities are represented in the *top-form* of Grassmannian integrals in which the integrands are comprised of rational functions of minors of the constraint matrices $\{\mathbf{R}(M_C)\}$. The top-form is elegant in that the amplitude structures are simple and compact; and the Yangian symmetry is manifest in the positive diffeomorphisms of positive Grassmannian geometry [3]. It is therefore crucial to express scattering amplitudes in top-form in order to explore its power to further uncover hidden symmetries and dualities of the scattering amplitudes. We present in this letter our successful construction of top-forms for non-planar scattering amplitudes, building on our earlier work of uncovering the first class of nonplanar Yangian permutation relations [17]. Our method applies to multi-loop, beyond-MHV leading singularities.

Exciting recent progress in $\mathcal{N} = 4$ SYM scattering amplitudes computation (by the on-shell method) is reported by many research groups in [2, 17, 18, 20, 21, 28, 43, 45, 46]; together we have made a step forward in the computation of nonplanar $\mathcal{N} = 4$ SYM scattering amplitudes, and hopefully in the formulation of AdS/CFT correspondence at finite N .

BCFW decompositions of leading singularities

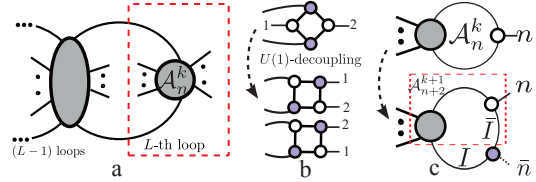


FIG. 1. (a) Obtaining the L -th loop amplitude recursively. (b) Utilising the $U(1)$ decoupling relation to turn a nonplanar diagram into a planar one. (c) Introduction of an auxiliary external momentum line to form the BCFW bridge.

The aim of this work is to obtain a simple and compact analytical expression—valid for arbitrary number of loops—of leading singularities of scattering amplitudes beyond the planar limit. A general leading singularity can be represented by a reduced on-shell diagram. BCFW bridge decomposition provides an efficient way of constructing on-shell diagram, at least in the planar limit. In non-planar cases, we can obtain the BCFW bridge decomposition chain by extracting planar sub-diagrams and compute them recursively [18, 19] as shown in Fig. 1. For the sub-diagrams that are BCFW-decomposable, we perform according to the recipe presented in [18, 19]. There exist, however, “No Bridge” (NB) diagrams which do not contain any BCFW bridges [18, 21]. We present a method in [18, 19] to transform some NB-diagrams by applying $U(1)$ -decoupling relations, schematically depicted in Fig. 1 (b).

In this work we present a general method applicable to any NB-diagrams. The key is to add an auxiliary external momentum line to form an *auxiliary BCFW bridge*, shown in Fig. 1 (c). To regain the original NB diagram we take the soft limit [26, 27, 29], setting the auxiliary momentum to zero. In this way the BCFW decomposition chain of the reduced on-shell diagrams beyond the planar limit can be obtained.

In the rest of the letter we present a recipe for constructing an analytical expression, the *top-form*, for a nonplanar leading singularity using the BCFW bridge decomposition chain [18] after adding an auxiliary exter-

nal momentum line.

Construction of the top-form The top-form of an on-shell diagram is obtained once the geometric constraints, Γ , and the integrand, $f(C)$, are determined. A non-planar leading singularity in the form [3]

$$\mathcal{T} = \oint_{\Gamma} \frac{dC^{k \times n}}{\text{Vol}(GL(k))} \frac{\delta^{k \times 4}(C \cdot \tilde{\eta})}{f(C)} \delta^{k \times 2}(C \cdot \tilde{\lambda}) \delta^{2 \times (n-k)}(\lambda \cdot C^{\perp}).$$

requires to calculate $f(C)$ and Γ under the BCFW shifts and take soft limit for the auxiliary BCFW bridges.

Let us study the BCFW shifts. The integrand, $f(C)$, must contain those poles equivalent to the constraints in Γ ; or the contour integration around Γ will vanish. Each BCFW bridge removes one pole in $f(C)$ by shifting a zero minor to be nonzero: in nontrivial cases the poles in the integrand must change their forms and the integrand changes its functional form accordingly. To see this we parametrize the constraint matrix, C , using the BCFW parameter, α . In a BCFW shift, a column vector X is shifted: $X \rightarrow \hat{X} = X + \alpha Y$, with several minors of $f(C)$ become functions of α . After the shift, there exists at least one constraint $M_0(X) = 0$ being shifted to $M_0(\hat{X}) = M_0(X) + \alpha R(Y)$ if there is a top-form. This is demonstrated in the following section. Meanwhile the factor $M_0(\hat{X})$ should be presented in the denominator to contribute a pole at $\alpha = 0$. In other words $\alpha = M_0(\hat{X})/R(Y)$ is then a rational function of \hat{C} and can be subtracted from other shifted minors to obtain some shift-invariant minors of \hat{C} , $M_i(X) = M_i(\hat{X} - \alpha Y)$. In summary, attaching a BCFW bridge, the integrand is,

$$f(\hat{C}) = M_0(\hat{X}) \prod_i M_i(\hat{X} - \alpha Y) \times \left(\begin{array}{c} \text{minors} \\ \text{without } \alpha \end{array} \right). \quad (1)$$

Now we discuss structures other than BCFW shifts in the NB diagrams [18, 21]. The top-form is obtained by imposing $U(1)$ -decoupling relation in [18]; in this work we focus on the auxiliary BCFW bridges. Top forms of those diagrams containing auxiliary BCFW bridges can be obtained using the above method. We discuss presently how they return to the top-forms of the original NB diagrams upon taking the soft limits.

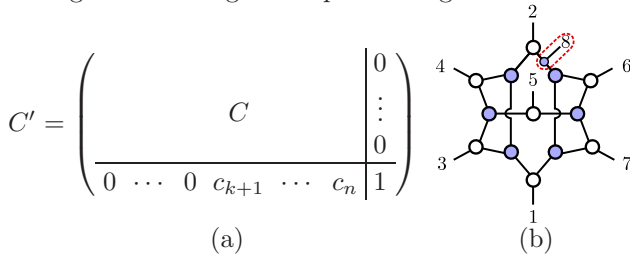


FIG. 2. A non-planar NMHV 4-loop leading singularity.

The on-shell diagram \mathcal{A}_{n+1}^{k+1} with one auxiliary line as shown in (c) of Fig.1 can be written in two equivalent

forms:

$$\int \frac{\mathcal{A}_{n+2}^{k+1} d\Omega_I \langle I\bar{I} \rangle^3}{\langle \bar{n}I \rangle^2 \langle \bar{I}\bar{n} \rangle} \delta([\bar{n}I]) \delta^4(\tilde{\eta}_{\bar{n}} + \frac{\langle \bar{I}\bar{n} \rangle}{\langle \bar{I}I \rangle} \tilde{\eta}_I), \quad (2)$$

$$\oint_{\Gamma} \frac{dC^{k \times n} d\vec{c}}{\text{Vol}(GL(k))} \frac{(1 \cdots k) \bar{\delta}}{f(C, c_i)} \delta^2(\sum_{i=k+1}^{n, \bar{n}} c_i \tilde{\lambda}_i) \delta^4(\sum_{i=k+1}^{n, \bar{n}} c_i \tilde{\eta}_i), \quad (3)$$

where $c_{\bar{n}} = 1$, $d\vec{c} = dc_{k+1} \cdots dc_n$, $\bar{\delta} = \delta^{k \times 4}(C \cdot \tilde{\eta}) \delta^{k \times 2}(C \cdot \tilde{\lambda}) \delta^{2(n-k)}(\lambda \cdot C^{\perp})$ and $d\Omega_I = \frac{d^2 \lambda_I d^2 \bar{\lambda}_I}{\text{vol}(GL(1))} d^4 \tilde{\eta}_I$. Eq.(2) is obtained directly from Fig.1(c) by integrating over the internal line \bar{I} . Eq.(3) is a general top-form of \mathcal{A}_{n+1}^{k+1} , where we choose a particular parametrisation of the Grassmannian matrix C' shown in Fig. 2(a). Our method of adding the auxiliary line can be justified by comparing (2) and (3). Noting that $\delta^2(\sum_{i=k+1}^{n, \bar{n}} c_i \tilde{\lambda}_i)$ is equivalent to $\delta(\sum_{i=k+1}^n c_i \frac{[i1]}{[\bar{n}1]} + 1) \delta([\bar{n}I])$, (2) and (3) can be proved to both contain the term $\delta([\bar{n}I]) \delta^4(\tilde{\eta}_{\bar{n}} + \frac{\langle \bar{I}\bar{n} \rangle}{\langle \bar{I}I \rangle} \tilde{\eta}_I)$ which can be removed from the overall constraint delta function. The remaining part of (2) corresponds to the NB diagram \mathcal{A}_n^k under the limit $\lambda_{\bar{n}} \rightarrow 0$. On the other hand, after taking the soft limit (3) yields

$$\mathcal{A}_n^k = \oint_{\Gamma} \frac{dC^{k \times n} dc_{k+1} \cdots dc_n}{\text{Vol}(GL(k))} \frac{(1 \cdots k) \delta^{k \times 4}(C \cdot \tilde{\eta})}{f(C, c_i)} \times \delta^{k \times 2}(C \cdot \tilde{\lambda}) \delta^{2 \times (n-k)}(\lambda \cdot C^{\perp}) \delta(\sum_{i=k+1}^n c_i \frac{[i1]}{[\bar{n}1]} + 1). \quad (4)$$

This is easily proven by counting the degrees of freedom of the associated on-shell diagram in which only one element c_f among c_i is a free parameter. As we shall prove in the following section, NB diagrams having top-forms requires that $c_i/c_f = \mathbf{R}(M_C)$. Using this relation, the integration $\int \frac{dc_f}{c_f} \delta(\sum_{i=k+1}^n c_i \frac{[i1]}{[\bar{n}1]} + 1)$ gives 1. Finally we obtain the top-form of \mathcal{A}_n^k upon expanding the minors of C' into C minors in the integrand.

An NMHV NB diagram example: We demonstrate the construction of top-form for the NB diagrams in an NMHV four loop example Fig. 2(b) (MHV example is discussed in [21], see also Appendix). Leg 8 is the auxiliary line added. The constraints in C' are $(1234)^3, (345)^2, (567)^2$. These constraints impose three independent linear relations on the four parameters shown in Fig. 2(a), therefore only one free parameter remains which leaves no extra coefficients after the contour integration: Minors in C' coincide with those in C . The top-form integrand of the NMHV diagram is

$$\frac{1}{f} = \frac{1}{f_{\text{planar}}} \times \frac{-(134)(467)^2(125)^3}{(124)(126)(135)(145)(267)(457)},$$

where $f_{\text{planar}} = (123)(234)(345)(456)(567)(671)(712)$; the geometry constraints in C is $(345)^2, (567)^2$.

Another example with tangled geometric constraints At multi-loop level the geometric constraints for

a nonplanar leading singularity can be highly tangled as the diagrams cannot, in general, be reduced to the planar ones by KK-relation [49]. Consider a nonplanar 2-loop diagram \mathcal{A}_6^3 in Fig.(3), the last bridge attached yields a tangled geometric constraint. Its exact expression can be obtained by transforming linearly the constraints in the last step, $(234) = 0$, $\frac{(234)}{(214)} - \frac{(356)}{(156)} = 0$. Adding the bridge $(1, 3)$ eliminates $(234) = 0$ and leaves $\frac{(234)}{(214)} - \frac{(356)}{(156)} = 0$ invariant, resulted in a tangled constraint, $((1\hat{3}) \cap (24)56)$.

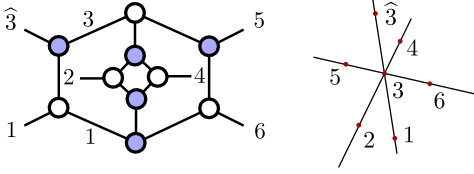


FIG. 3. An example of nonplanar two-loop diagram \mathcal{A}_6^3 . In projective space its constraint $((1\hat{3}) \cap (24)56)$ means line $(1\hat{3})$, line (24) and line (56) all intersecting at Point 3. The top-form integrand before attaching the last BCFW bridge is [3, 18],

$$\frac{1}{f} = \frac{(361)}{(123)(234)(345)(356)(146)(561)(612)}.$$

The last attachment of Bridge $(1, 3)$ seems to eliminate two poles in the denominator at the same time. Applying the same linear transformation to the denominator:

$$\frac{1}{(234)(356)} \rightarrow \frac{-1}{(2\hat{3}4) \left(\frac{-(156)(234)}{(214)} + (356) \right)}, \text{ we obtain}$$

$$\frac{1}{f} = \frac{(214)^2(361)}{(123)(234)((13) \cap (24)56)((13) \cap (24)45)(146)(561)(612)},$$

where the integration contour Γ is around the pole (234) .

Rational top-forms, linear BCFW-bridges and rational soft limit: Attaching BCFW-bridges or auxiliary BCFW-bridges, using the 3- or 4-point amplitude, all non-planar diagrams can be constructed and their $d\log$ forms found. We should stress, however, that not all non-planar on-shell diagrams have rational top-forms; and it is worth to remark on which kind of nonplanar on-shell diagrams can have rational top-forms. We address this question by building up an equivalent relation between *rational top-form*, and *linear BCFW bridges* (with *rational soft limit*). If an addition of a BCFW-bridge results in the shifted constraint function, f' , being a linear function of α , we call this BCFW bridge a *linear BCFW bridge*. If the soft limit of auxiliary line leads to additional constraints such that $\frac{c_i}{c_j}$ being a rational function of C -minors for all non-vanishing c_i in the added row of C' , we call this soft limit a *rational soft limit*.

A constraint function F_i is a rational function of minors of the Grassmannian matrix, C . Altogether they span an algebraic ideal $\mathcal{I}\{F_i\}$. Under a BCFW-shift $X \rightarrow \hat{X} = X + \alpha Y$, a constraint is eliminated, with C being transformed to \hat{C} . The transformed $f'(\hat{C})$ is also rational if α is also a rational function of \hat{C} .

Next we need to show that the rationality of α is guaranteed by the linear BCFW shifts. To prove their equivalence, assuming $\alpha = P(\hat{C})/Q(\hat{C})$, where P, Q are polynomials of minors of \hat{C} . Expanding P, Q as polynomials of α as well as the minors of C ,

$$\alpha = \frac{P_0 + P_1\alpha + P_2\alpha^2 + \dots + P_N\alpha^N}{Q_1 + Q_2\alpha + \dots + Q_N\alpha^{N-1}}.$$

The coefficient in each power of α , such as $P_0, P_1 - Q_1, P_2 - Q_2, \dots, P_N - Q_N$, is supposed to vanish. If any of them appears nonzero, it must fall into the ideal $\mathcal{I}\{F_i\}$. This means that all the coefficients are constraints of C . Under the shift, P_i and Q_i become $\hat{P}_i = P_i + \sum_{j=1}^{N-i} \binom{j}{i+j} P_{i+j} \alpha^j$ and $\hat{Q}_i = Q_i + \sum_{j=1}^{N-1-i} \binom{j}{i+j} P_{i+j} \alpha^j$. The constraint $P_N - Q_N$ remains the same after the shift $\hat{P}_N - \hat{Q}_N = P_N - Q_N$. The constraint $P_{N-1} - Q_{N-1} = 0$ appears linearly dependent on α upon

$$\hat{P}_{N-1} - \hat{Q}_{N-1} = [NP_N - (N-1)Q_N]\alpha.$$

If $[NP_N - (N-1)Q_N]$ does not vanish then the constraint $P_{N-1} - Q_{N-1} = 0$ is the removed. Otherwise $P_N = Q_N = 0$ and the constraint $P_{N-2} - Q_{N-2} = 0$ is shifted linearly, $\hat{P}_{N-2} - \hat{Q}_{N-2} = [(N-1)P_{N-1} - (N-2)Q_{N-1}]\alpha$. Since $P(\hat{C})$ cannot be totally independent of α , we can trace the constraints from N to 0 until we find one constraint $(P_i - Q_i)$ which is a linear function of α after a shift. This constraint is then the constraint being removed.

The proof of the reverse is straightforward: if one constraint becomes a linear function of α under a shift, for instance $F_i(C) \rightarrow F_i(\hat{C}) = F_i(C) + F'_i(C)\alpha = F'_i(\hat{C})\alpha$ where $F_i(C)$ vanishes and $F'_i(C)$ is invariant under the shift, we have $\alpha = F_i(\hat{C})/F'_i(\hat{C})$. Note that the remaining $s-1$ constraints can be written in the form $F_i(\dots \hat{X} - \alpha Y \dots) = 0$, for $i \in [2, s]$, which are invariant under the shift.

The NB diagrams constructed by the linear (auxiliary) BCFW-bridge and the rational soft limit can have rational top-forms. The C matrix parameters α_C that can be denoted by $\mathbf{R}(M_C)$ is also $\mathbf{R}(M_{C'})$. The additional C' elements c_i are of form $c_i \mathbf{R}(\alpha_C)$ (indicating a rational soft limit for $c_i \neq 0$). Since c_i is naturally $\mathbf{R}(M_{C'})$, all free parameters in C' are then rational functions of minors, i.e., the top-form is rational. Inversely, given the linear auxiliary bridge and rational soft limit, any C parameter denoted by $\mathbf{R}(M_{C'})$ can be expanded to $\mathbf{R}(M_C)$ directly.

A Geometric approach to obtain the constraints systematically: For a NB diagram, obtaining the C matrix geometry from C' is straightforward: $(i_1 \dots i_k \bar{n})_{C'}^k \mapsto (i_1 \dots i_k)_{C'}^{k-1}$ and $(i_1 \dots i_s)_{C'}^{s-1} \mapsto (i_1 \dots i_s)_{C'}^{s-1}$ for $s \leq k$. Hence we only need to discuss the geometric transformations under adding one (auxiliary) BCFW-bridge. The general algebraic forms of the constraints encoded in on-shell diagrams can now be readily obtained. Geometrically each constraint is interpreted as a point lying on a hyperplane. When we

attach a BCFW-bridge, $X \rightarrow \hat{X} = X + \alpha Y$. In the simplest case only one geometric relation is affected, e.g. $(XA_1A_2 \dots A_{i_1})^{i_1} \mapsto (XYA_1A_2 \dots A_{i_1})^{i_1+1}$ for $i_1+1 \leq k$ (If $i_1+1 = k$ there is no constraint.). A more complicated case would be two constraints $(XA_1A_2 \dots A_{i_1})^{i_1}$ and $(XB_1B_2 \dots B_{i_2})^{i_2}$ both containing the shifting leg. Upon attaching a BCFW-bridge a tangled constraint results:

$$\alpha = \frac{V^{i_1+1}(\hat{X}A_1 \dots A_{i_1})}{V^{i_1+1}(YA_1 \dots A_{i_1})} = \frac{V^{i_2+1}(\hat{X}B_1 \dots B_{i_2})}{V^{i_2+1}(YB_1 \dots B_{i_2})}, \quad (5)$$

where V stands for the volume of the hyperpolyhedron. It is indeed a geometric constraint on the Grassmannian manifold—the intersection point of one line and one hyperplane lying on another hyperplane: $((\hat{X}Y) \cap (B_1B_2 \dots B_{i_2})A_1A_2 \dots A_{i_1})$. We denote the intersection point of $(\hat{X}Y) \cap (B_1B_2 \dots B_{i_2})$ as $Q = C_1\hat{X} + C_2Y$. Since Q also lies in the plane $(B_1B_2 \dots B_{i_2})$, $C_1V^{i_2+1}(\hat{X}B_1B_2 \dots B_{i_2}) + C_2V^{i_2+1}(YB_1B_2 \dots B_{i_2}) = 0$. Thus the initial constraint $(QA_1A_2 \dots A_{i_1})^{i_1}$ directly yields (5). One may have noticed that the point Q is precisely the point X before shifting. If we go on attaching another bridge that involves this tangled constraint, the set of constraints can again be written as minors of the Grassmannian matrix.

Therefore we conclude that general constraints can always be labelled using nested spans and intersections. Consider attaching a linear BCFW bridge (Y, X) in an arbitrary amplitude, a constraint to be shifted is

$$M(X) \equiv \left(\dots (XA_1^{(0)} \dots A_{a_0}^{(0)}) \cap (B_1^{(1)} \dots B_{b_1}^{(1)})A_1^{(1)} \dots A_{a_1}^{(1)} \dots \right. \\ \left. \cap (B_1^{(m)} \dots B_{b_m}^{(m)})A_1^{(m)} \dots A_{a_m}^{(m)} \right), \quad (6)$$

with X being the external line to be shifted, $A^{(\cdot)}$ and $B^{(\cdot)}$ denoting the two sets of external lines. If column $X \in \text{Set}[A^{(\cdot)}]$ or $X \in \text{Set}[B^{(\cdot)}]$, they can be freely replaced by \hat{X} after attaching the bridge involving X . Otherwise the constraint will be a nonlinear function of α , resulting in an irrational top-form. We present a counter example in Appendix to illustrate this point. We can then simplify $M(X)$ as follows $(L^{(m)}(X) \cap (B_1^{(m)} \dots B_{b_m}^{(m)})A_1^{(m)} \bar{A}_2^{(m)} \dots \bar{A}_{a_m}^{(m)})$, where $\bar{A}^{(\cdot)}$ are some points or hyperplanes spanned by $A^{(\cdot)}$ and $B^{(\cdot)}$, which are in turn governed by a simple relation, $(A_1A_2A_3) \cap P = (((A_1A_2) \cap P)((A_2A_3) \cap P)) = (((A_1A_2) \cap P)\bar{A})$. After the shift the constraint $M(X)$ is removed. In order to obtain the other constraints, we look for the \hat{C} representation of X . This is achieved by unfolding the nested intersections one level by one level.

To write a constraint in a compact form and manifest the geometric relations encoded, we define a line $L(X)$, for $i \in [2, m]$

$$L^{(i)}(X) \equiv (L^{(i-1)}(X) \cap (B_1^{(i-1)} \dots B_{b_{i-1}}^{(i-1)})A_1^{(i-1)}).$$

We further define a point

$$R^{(i)}(X) \equiv L^{(i)}(X) \cap (B_1^{(i)} \dots B_{b_i}^{(i)}),$$

where $i \in [2, m]$. Given a minor $M(X)$, we could obtain $R^{(m)}(X)$ as

$$R^{(m)}(X) = L^{(m)}(\hat{X}Y) \cap (B_1^{(m)} \dots B_{b_m}^{(m)}) \cap (A_1^{(m)} \dots \bar{A}_{a_m}^{(m)}).$$

All levels in $R^{(i)}(X)$ can be recursively obtained according to

$$R^{(i-1)} = (R^{(i)}A_1^{(i-1)}) \cap (L^{(i-1)}(\hat{X}Y) \cap (B_1^{(i-1)} \dots B_{b_{i-1}}^{(i-1)})).$$

The geometric relations are shown in Fig. 4. Finally we are able to denote the column X using the columns in the shifted Grassmannian, $X = (R^{(1)}A_1^{(0)}) \cap (\hat{X}Y)$. After removing the constraint $M(X) = 0$, the remaining constraints are invariant under the \hat{C} representation of X , making them independent of the shift (Y, X) .

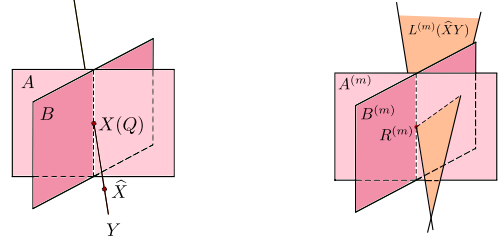


FIG. 4. (a)(b)

SUMMARY AND OUTLOOK

We have obtained the top-form integrands for nonplanar leading singularities by BCFW-decompositions. In the cases that one cannot attach a BCFW-bridge we can add an auxiliary external momentum line judiciously to enable the application of the chain of BCFW-decompositions and taking the soft limit on the auxiliary momentum line to recover the original diagrams. This combination of strategies can successfully compute leading singularity contributions for nonplanar diagrams of arbitrary loops. We have also classified nonplanar on-shell diagrams according to whether they possess rational top-forms, and proved its equivalence to linear BCFW bridges (and rational soft limit for diagrams with no external BCFW-bridges). With the chain of BCFW-bridge decompositions obtained rational top-forms of the nonplanar on-shell diagrams can be derived in a straightforward way. This method applies to leading singularities of nonplanar multi-loop amplitudes beyond MHV.

An immediate question is whether all on-shell diagrams representing nonplanar leading singularities belong to this class, so that all leading singularities can be expressed in rational top-forms.

Top-form, being simple and compact, is a great tool to uncover hidden symmetries (e.g. Yangian symmetry beyond planarity [17]) which are otherwise highly tangled

in nonplanar leading singularities. When combined with generalised unitarity cuts, top-form holds promise in constructing the integrals as well as revealing the symmetries and dualities of loop-level scattering amplitudes.

Mathematically our method of performing the BCFW decompositions is related to the toric geometry arisen in the characterisation of Matroid Stratification. Further exploration on the relationship between BCFW decompositions and Matroid Stratification will also shed light on the geometry of underlying Grassmannian manifolds.

APPENDIX

All rational top-forms can be constructed by our method described above. In our discussion we have assumed that the BCFW bridges are the *linear BCFW bridges*—each successive α -shift transforms the constraints linearly and can thus be represented by a rational function of minors of the underlying constraint C-matrix. However not all on-shell diagrams are made up completely of such bridges: the constraints can be nonlinear in α and cannot be written as rational functions under some shift. Such an on-shell diagram will not have a rational top-form.

We present a counter example, \mathcal{A}_{10}^4 . Upon attaching the bridge (3,4), two constraints $(2,3,4,8)^3$ and $(1,3,4,6)^3$ emerge (the superscripts denote the number of independent column vectors), with two columns, 3 and 4, being the same. Attaching the bridge (5,3), one of the constraints is removed and the other one becomes $((5,3) \cap (2,4,8), 1, 4, 6)^3$. If we go on attaching the bridge (7,4), the tangled constraint is removed. However, due to the column 4 appearing twice in that constraint, such a bridge results in a nonlinear shift of the algebraic ideal. Therefore such a α -shift cannot be represented linearly by some minor being zero, violating our linearity requirements in the construction of rational top-forms.

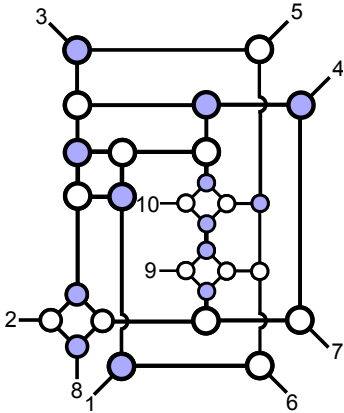


FIG. 5. A non-planar diagram of \mathcal{A}_{10}^4

TABLE I. The evolution of the geometric constraints with adding BCFW bridges for the diagram in Fig. 5.

	$(3)^0$	$(4)^0$	$(7)^0$	$(8)^0$	$(9)^0$	$(10)^0$
(6, 10)	$(3)^0$	$(4)^0$	$(7)^0$	$(8)^0$	$(9)^0$	$(6, 10)^1$
(2, 6)	$(3)^0$	$(4)^0$	$(7)^0$	$(8)^0$	$(9)^0$	$(2, 6, 10)^2$
(6, 9)	$(3)^0$	$(4)^0$	$(7)^0$	$(8)^0$	$(6, 9)^1$	$(2, 6, 10)^2$
(5, 6)	$(3)^0$	$(4)^0$	$(7)^0$	$(8)^0$	$(5, 6, 9)^2$	$(2, 6, 10)^2$
(6, 9)	$(3)^0$	$(4)^0$	$(7)^0$	$(8)^0$	$(5, 6, 9)^2$	$(2, 6, 9, 10)^3$
(6, 8)	$(3)^0$	$(4)^0$	$(7)^0$	$(6, 8)^1$	$(5, 6, 9)^2$	$(2, 6, 9, 10)^3$
(6, 7)	$(3)^0$	$(4)^0$	$(6, 7)^1$	$(6, 8)^1$	$(5, 6, 9)^2$	$(2, 6, 9, 10)^3$
(5, 6)	$(3)^0$	$(4)^0$	$(7, 8)^1$	$(5, 6, 8)^2$	$(5, 8, 9)^2$	$(2, 8, 9, 10)^3$
(2, 5)	$(3)^0$	$(4)^0$	$(7, 8)^1$	$(6, 8, 9)^2$	$(2, 5, 8, 9)^3$	$(2, 8, 9, 10)^3$
(2, 4)	$(3)^0$	$(2, 4)^1$	$(7, 8)^1$	$(6, 8, 9)^2$	$(2, 5, 8, 9)^3$	$(2, 8, 9, 10)^3$
(1, 2)	$(3)^0$	$(1, 2, 4)^2$	$(7, 8)^1$	$(6, 8, 9)^2$	$(4, 5, 8, 9)^3$	$(4, 8, 9, 10)^3$
(2, 3)	$(2, 3)^1$	$(1, 2, 4)^2$	$(7, 8)^1$	$(6, 8, 9)^2$	$(4, 5, 8, 9)^3$	$(4, 8, 9, 10)^3$
(1, 2)	$(1, 2, 3)^2$	$(1, 3, 4)^2$	$(7, 8)^1$	$(6, 8, 9)^2$	$(4, 5, 8, 9)^3$	$(4, 8, 9, 10)^3$
(8, 2)	$(1, 2, 3, 8)^3$	$(1, 3, 4)^2$	$(7, 8)^1$	$(6, 8, 9)^2$	$(4, 5, 8, 9)^3$	$(4, 8, 9, 10)^3$
(2, 8)	$(1, 2, 3, 8)^3$	$(1, 3, 4)^2$	$(2, 7, 8)^2$	$(6, 7, 9)^2$	$(4, 5, 7, 9)^3$	$(4, 7, 9, 10)^3$
(6, 1)	$(2, 3, 4, 8)^3$	$(1, 3, 4, 6)^3$	$(2, 7, 8)^2$	$(6, 7, 9)^2$	$(4, 5, 7, 9)^3$	$(4, 7, 9, 10)^3$
(3, 4)	$(2, 3, 4, 8)^3$	$((5, 3) \cap (2, 4, 8), 1, 4, 6)^3$	$(2, 7, 8)^2$	$(6, 7, 9)^2$	$(5, 7, 9, 10)^3$	
(5, 3)		$(1, 4, 6)^3$	$(2, 7, 8)^2$	$(6, 7, 9)^2$	$(5, 7, 9, 10)^3$	
(7, 4)			$(2, 7, 8)^2$	$(6, 7, 9)^2$	$(5, 7, 9, 10)^3$	

An MHV example

A six-point three-loop MHV example have been analysed in [21]. Here, for comparison, we provide our calculation by attaching the auxiliary BCFW-bridges. We attach an auxiliary external momentum line, in Fig.6, and form an auxiliary BCFW-bridge (3,7). This on-

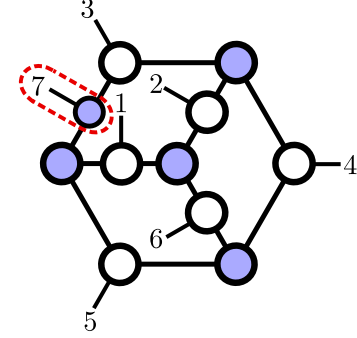


FIG. 6. An MHV example

shell diagram can be decomposed to identity as follows, $(1, 7) \rightarrow (2, 6) \rightarrow (3, 5) \rightarrow (2, 3) \rightarrow (3, 4) \rightarrow (12) \rightarrow (2, 3) \rightarrow (5, 7) \rightarrow (3, 7)$. Before adding Bridge-(5, 7), the on-shell diagram is still planar. The Grassmannian constraints and the top-form can be obtained directly from the permutation [3] shown in the first row of Tab.II. Adding Bridge-(5, 7), the constraint $(71)^1 \rightarrow (157)^2$, as shown in the second row of Tab.II. Adding Bridge-(3, 7), the constraint $(157)^2$ disappears. Before attaching Bridge-(5, 7), the top-form is

$$\frac{1}{(123)(234)(345)(456)(567)(671)(712)}$$

When attaching (5, 7), the contour integral around the pole $(712) = (\tilde{7}12) - \alpha(512)$ is replaced by $\frac{d\alpha}{\alpha}$ with $\alpha =$

TABLE II. The evolution of the geometric constraints.

	$(71)^1$	$(234)^2$	$(456)^2$	$(612)^2$
$(5, 7)$	$(157)^2$	$(234)^2$	$(456)^2$	$(126)^2$
$(3, 7)$		$(234)^2$	$(456)^2$	$(126)^2$

$\frac{(\widehat{712})}{(512)}$. All the minors except (712) with column 7 may be affected by the bridge

$$\begin{aligned} (567) &\rightarrow \frac{(56(\widehat{75}) \cap (12))}{(512)} = \frac{(56\widehat{7})}{(512)} \\ (671) &\rightarrow \frac{(6(\widehat{75}) \cap (12)1)}{(512)} = \frac{(\widehat{715})(126)}{(512)}. \end{aligned}$$

Then the top-form integrand becomes

$$\frac{(125)}{(123)(234)(345)(456)(567)(157)(126)(127)}.$$

Similarly after attaching Bridge-(3, 7) the top-form integrand becomes

$$\frac{(135)^2}{(123)(234)(345)(456)(156)(357)(157)(126)(137)}.$$

To obtain the top-form of the original diagram, we parametrize the C' as

$$\left(\begin{array}{c|c} C & \begin{matrix} 0 \\ 0 \\ 1 \end{matrix} \\ \hline 0 & 0 \quad c_3 \quad c_4 \quad c_5 \quad c_6 \end{array} \right).$$

Then we expand all the minors in C' as those of C

$$\begin{aligned} (126) &= (12)c_6 & (234) &= -c_3(24) + c_4(23) \\ (123) &= (12)c_3 & (456) &= c_4(56) - c_5(46) \\ (156) &= -(16)c_5 & (135) &= -c_3(15) + c_5(13) \\ (137) &= (13) & (345) &= c_3(45) - c_4(35) + c_5(34) \\ (357) &= (35) & (157) &= (15), \end{aligned}$$

The top-form becomes

$$\begin{aligned} &\frac{(-c_3(15) + c_5(13))^2}{-(12)(35)(15)(12)(13)(16)c_3c_6c_5(-c_3(24) + c_4(23))} \\ &\times \frac{1}{(c_3(45) - c_4(35) + c_5(34))(c_4(56) - c_5(46))}. \end{aligned}$$

The additional pole is characterised by $(126), (234), (456)$. Upon contour integration gives $c_6 \rightarrow 0, c_3 \rightarrow \frac{(23)}{(24)}c_4, c_5 \rightarrow \frac{(56)}{(46)}c_4$ and

$$\frac{[(56)(13)(24) - (23)(15)(46)]^2}{(23)(12)(24)(26)(45)(34)(16)(56)(35)(15)(13)(46)},$$

consistent with the MHV example in[21]. This can be simplified further,

$$\begin{aligned} &-f_p(125364) + f_p(125463) - f_p(134265) \\ &+ f_p(126543) - f_p(132465) - f_p(123564), \end{aligned}$$

with f_p denoting the planar amplitudes of the corresponding orders.

An \overline{MHV} example

In this subsection we give an example of a different situation—an auxiliary line connected to a white vertex—using an \overline{MHV} example (Fig.7) for illustration. Attaching an auxiliary line enables the BCFW-decomposition to identity by the following chain: $(7, 3) \rightarrow (7, 5) \rightarrow (3, 4) \rightarrow (2, 3) \rightarrow (4, 5) \rightarrow (3, 4) \rightarrow (1, 3) \rightarrow (4, 6) \rightarrow (3, 7)$. Before adding Bridge-(7, 5) the on-shell diagram is planar. The Grassmannian constraints (the first row of Tab.III) and the top-form can be obtained directly from the permutation[3]:

$$\frac{1}{(1234)(2345)(3456)(4567)(5671)(6712)(7123)}.$$

FIG. 7. An \overline{MHV} example

TABLE III. Geometric constraints

	$(2(345)^26)^3$	$(345)^2$	$(5671)^3$	$(7123)^3$
$(7, 5)$	$(2346)^3$	$(3457)^3$	$(5671)^3$	$(7123)^3$
$(7, 3)$		$(3457)^3$	$(5671)^3$	$(7123)^3$

The transformation of constraints after adding the bridges $(7, 5)$ and $(7, 3)$ is shown in the second and third rows of Tab.III; the top-form of \mathcal{A}_7^4 becomes:

$$\frac{-(2467)^2}{(2347)(1246)(2456)(3457)(2346)(4567)(1567)(1267)(1237)}$$

Without losing of generality, we choose the first four columns of \widehat{C} matrix as identity:

$$\begin{pmatrix} \mathbf{e}_1 & \mathbf{e}_2 & \mathbf{e}_3 & \mathbf{e}_4 & \vec{c} \\ 1 & 0 & 0 & 0 & * & * & c_1 \\ 0 & 1 & 0 & 0 & * & * & c_2 \\ 0 & 0 & 1 & 0 & * & * & c_3 \\ 0 & 0 & 0 & 1 & * & * & c_4 \end{pmatrix}$$

Then the last column can be represented by column one to four as:

$$\vec{c} = c_1\mathbf{e}_1 + c_2\mathbf{e}_2 + c_3\mathbf{e}_3 + c_4\mathbf{e}_4.$$

In this way we can rewrite the minor with column-7 as:

$$\begin{aligned}(1237) &= c_4(1234) & (1567) &= c_2(1256) + c_3(1356) \\ (1267) &= c_3(1263) & (2467) &= c_1(2461) + c_3(2463) \\ (2347) &= c_1(1243) & (3457) &= -c_1(1345) - c_2(2345) \\ (4567) &= -c_1(1456) - c_2(2456) - c_3(3456)\end{aligned}$$

Consider the three poles of \mathcal{A}_7^4 , since there is no constraint in \mathcal{A}_6^4 we should integrate around all of the three poles and removing three coefficients. At last, there is only one coefficient left and others can be represented by it: $c_4 \rightarrow 0, c_1 \rightarrow -\frac{(2345)}{(1345)}c_2, c_3 \rightarrow -\frac{(1256)}{(1356)}c_2$. The remaining coefficient in the top-form is $\frac{dc_2}{c_2}$ and can be fixed by one of the columns in \widehat{C}^\perp (noting that \widehat{C}^\perp have one more column than C^\perp , which can be removed directly). Finally, the top-form of \mathcal{A}_6^4 is:

$$\frac{1}{f_p} \frac{-(2345)(1246)(1356) - (1256)(2346)(1345)]^2}{(1246)(2456)(1345)(2346)(1356)(1235)},$$

where $f_p = (1234)(2345)(3456)(4561)(5612)(6123)$. This can also be simplified as

$$\begin{aligned}-f_p(142356) - f_p(143265) + f_p(132456) \\ -f_p(132654) + f_p(123465) - f_p(123465).\end{aligned}$$

More details on the NMHV NB diagram:

In this subsection we present the gory details in the calculation and simplification in the NMHV example (Fig.2(b)). Since this diagram cannot be decomposed by BCFW-bridges directly we introduce an auxiliary external momentum line the leg-8. The diagram transforms to planar one by removing the bridges (2, 8), (6, 8) and (4, 2). The total decomposition chain is (2, 8) \rightarrow (6, 8) \rightarrow (4, 2) \rightarrow (1, 2) \rightarrow (2, 3) \rightarrow (2, 4) \rightarrow (4, 5) \rightarrow (4, 6) \rightarrow (6, 7) \rightarrow (1, 6) \rightarrow (6, 8).

Before adding Bridge-(4, 2) the planar diagram top-form is

$$\frac{1}{(1234)(2345)(3456)(4567)(5678)(6781)(7812)(8123)}$$

with constraints shown in the first row of Tab. IV. After

TABLE IV. Geometric constraints evolution for NMHV example

	$(123)^2$	$(345)^2$	$(567)^2$	$(781)^2$
(4, 2)	$(1234)^3$	$(345)^2$	$(567)^2$	$(781)^2$
(6, 8)	$(1234)^3$	$(345)^2$	$(567)^2$	$(6781)^3$
(2, 8)	$(1234)^3$	$(345)^2$	$(567)^2$	

attaching all the BCFW bridges, we obtain the top-form integrand,

$$\frac{1}{(1234)(2345)(3456)(4567)(1567)(8672)(6781)} \times \frac{(1347)(6721)^3}{(7812)(3167)(1237)(1247)(1286)} \quad (7)$$

with geometry constraint as shown in the last row of Tab.IV. Then we expand the rank-4 minors into rank-3 minors

$$\begin{aligned}(1234) &= (123)c_4 & (2345) &= -(235)c_4 + (234)c_5 \\ (1237) &= (123)c_7 & (3167) &= -(317)c_6 + (316)c_7 \\ (1286) &= -(126) & (6721) &= -(721)c_6 + (621)c_7 \\ (8672) &= -(672) & (3456) &= (356)c_4 - (346)c_5 \\ (6781) &= -(671) & (1347) &= -(137)c_4 + (134)c_7 \\ (7812) &= (712) & (1247) &= -(127)c_4 + (124)c_7 \\ (1567) &= (167)c_5 - (157)c_6 + (156)c_7 \\ (4567) &= (467)c_5 - (457)c_6 + (456)c_7.\end{aligned}$$

Solving all the additional constraint incurred from the auxiliary line and vertex we get $c_4 \rightarrow 0, c_5 \rightarrow 0, c_7 \rightarrow \frac{(457)}{(456)}c_6$ and the final top-form intergrand

$$\frac{1}{f_p} \frac{(134)(357)[(457)(126) - (456)(127)]^3}{(124)(126)(135)(145)(267)(367)(457)^2},$$

where $f_p = (123)(234)(345)(456)(567)(671)(712)$. Using the Plucker relations the integrand $\frac{1}{f(C)}$ is

$$\begin{aligned}&\frac{(125)}{(124)(126)(167)(235)(257)(143)(345)(567)} \\ &+ \frac{(125)}{(124)(127)(165)(235)(267)(143)(345)(567)} \\ &+ \frac{(125)}{(123)(126)(167)(234)(145)(257)(345)(567)} \\ &+ \frac{(125)}{(123)(127)(165)(234)(145)(267)(345)(567)}.\end{aligned} \quad (8)$$

To further simplify the form it is hard to using the Plucker relations directly. A simpler technique is to parametrize the C matrix as

$$\begin{pmatrix} 1 & 2 & 3 & 4 & 5 & 6 & 7 \\ * & * & * & * & 0 & * & * \\ * & * & * & * & 0 & * & * \\ c_1 & c_2 & c_3 & 0 & 1 & 0 & c_7 \end{pmatrix}$$

and expand the three-column minor in the two-column

minor, and then the first term in (8) can be written as

$$\begin{aligned}
& \frac{-(12)(36)}{(124)(126)c_7(16)(23)(27)c_3(14)(34)(67)(36)} \\
&= \frac{-1}{(124)(126)(27)c_3(14)(34)(67)c_7(36)} \\
&+ \frac{1}{(124)(126)c_7(16)(37)c_3(24)(34)(67)} \\
&= \frac{-1}{(124)(126)(257)(134)(345)(567)(367)} \\
&- \frac{1}{(124)(126)(167)(234)(357)(345)(567)}. \quad (9)
\end{aligned}$$

Similarly we can rewrite the second term to forth term in (8) as

$$\begin{aligned}
(II) &= \frac{1}{(124)(127)(167)(346)(235)(345)(567)} \\
&+ \frac{1}{(124)(127)(134)(267)(356)(345)(567)}; \quad (10)
\end{aligned}$$

$$\begin{aligned}
(III) &= \frac{1}{(123)(126)(143)(467)(275)(345)(567)} \\
&+ \frac{1}{(123)(126)(243)(467)(175)(345)(567)}; \quad (11)
\end{aligned}$$

$$\begin{aligned}
(IV) &= \frac{1}{(123)(127)(143)(267)(456)(345)(567)} \\
&+ \frac{1}{(123)(127)(234)(167)(456)(345)(567)}. \quad (12)
\end{aligned}$$

* gang.chern@gmail.com

† cheung@nju.edu.cn

- [1] A. Postnikov, ArXiv Mathematics e-prints (2006), math/0609764.
- [2] S. Franco, D. Galloni, and A. Mariotti, Journal of High Energy Physics **2014**, 1 (2014).
- [3] N. Arkani-Hamed, J. L. Bourjaily, F. Cachazo, A. B. Goncharov, A. Postnikov, *et al.*, (2012), arXiv:1212.5605 [hep-th].
- [4] N. Arkani-Hamed, F. Cachazo, C. Cheung, and J. Kaplan, Journal of High Energy Physics **3**, 110 (2010), arXiv:0903.2110 [hep-th].
- [5] M. F. Paulos and B. U. W. Schwab, JHEP **1410**, 31 (2014), arXiv:1406.7273 [hep-th].
- [6] Y. Bai and S. He, (2014), arXiv:1408.2459 [hep-th].
- [7] T. Bargheer, Y. t. Huang, F. Loebbert and M. Yamazaki, “Integrable Amplitude Deformations for N=4 Super Yang-Mills and ABJM Theory,” Phys. Rev. D **91**, no. 2, 026004 (2015) [arXiv:1407.4449 [hep-th]].
- [8] L. Ferro, T. Lukowski, and M. Staudacher, (2014), arXiv:1407.6736 [hep-th].
- [9] S. Franco, D. Galloni, A. Mariotti, and J. Trnka, (2014), arXiv:1408.3410 [hep-th].
- [10] H. Elvang, Y.-t. Huang, C. Keeler, T. Lam, T. M. Olson, *et al.*, (2014), arXiv:1410.0621 [hep-th].
- [11] N. Arkani-Hamed, J. Bourjaily, F. Cachazo, and J. Trnka, Journal of High Energy Physics **2012**, 1 (2012).
- [12] N. Beisert, J. Henn, T. McLoughlin, and J. Plefka, Journal of High Energy Physics **4**, 85 (2010), arXiv:1002.1733 [hep-th].
- [13] J. Broedel, M. de Leeuw, and M. Rosso, JHEP **1406**, 170 (2014), arXiv:1403.3670 [hep-th].
- [14] J. Broedel, M. de Leeuw, and M. Rosso, (2014), arXiv:1406.4024 [hep-th].
- [15] N. Beisert, J. Broedel, and M. Rosso, Journal of Physics A: Mathematical and Theoretical **47**, 365402 (2014).
- [16] D. Chicherin, S. Derkachov, and R. Kirschner, Nuclear Physics B **881**, 467 (2014).
- [17] P. Du, G. Chen, and Y.-K. E. Cheung, Journal of High Energy Physics **2014**, 1 (2014).
- [18] B. Chen, G. Chen, Y. K. E. Cheung, Y. Li, R. Xie and Y. Xin, “Nonplanar On-shell Diagrams and Leading Singularities of Scattering Amplitudes,” arXiv:1411.3889 [hep-th].
- [19] B. Chen, G. Chen, Y. K. E. Cheung, R. Xie and Y. Xin, “Top-forms of Leading Singularities in Nonplanar Multi-loop Amplitudes,” arXiv:1506.02880 [hep-th].
- [20] Z. Bern, E. Herrmann, S. Litsey, J. Stankowicz, and J. Trnka, (2014), arXiv:1412.8584 [hep-th].
- [21] N. Arkani-Hamed, J. L. Bourjaily, F. Cachazo, A. Postnikov, and J. Trnka, (2014), arXiv:1412.8475 [hep-th].
- [22] S. Franco, D. Galloni, B. Penante, and C. Wen, (2015), arXiv:1502.02034 [hep-th].
- [23] S. J. Bidder, N. Bjerrum-Bohr, L. J. Dixon, and D. C. Dunbar, Physics Letters B **606**, 189 (2005).
- [24] A. Neitzke, Proceedings of the National Academy of Sciences **111**, 9717 (2014).
- [25] D. Xie and M. Yamazaki, Journal of High Energy Physics **2012**, 1 (2012).
- [26] Z. Bern, L. J. Dixon, D. C. Dunbar and D. A. Kosower, “One loop n point gauge theory amplitudes, unitarity and collinear limits,” Nucl. Phys. B **425**, 217 (1994) [hep-ph/9403226].
- [27] M. Bullimore, “Inverse Soft Factors and Grassmannian Residues,” JHEP **1101**, 055 (2011) [arXiv:1008.3110 [hep-th]].
- [28] N. Arkani-Hamed, J. L. Bourjaily, F. Cachazo, and J. Trnka, Phys.Rev.Lett. **113**, 261603 (2014), arXiv:1410.0354 [hep-th].
- [29] A. Volovich, C. Wen and M. Zlotnikov, “Double Soft Theorems in Gauge and String Theories,” arXiv:1504.05559 [hep-th].
- [30] P. Mastrolia, E. Mirabella, G. Ossola and T. Peraro, “Scattering Amplitudes from Multivariate Polynomial Division,” Phys. Lett. B **718**, 173 (2012) [arXiv:1205.7087 [hep-ph]].
- [31] P. Mastrolia and G. Ossola, “On the Integrand-Reduction Method for Two-Loop Scattering Amplitudes,” JHEP **1111**, 014 (2011) [arXiv:1107.6041 [hep-ph]].
- [32] B. Feng and R. Huang, Journal of High Energy Physics **2013**, 1 (2013).
- [33] Y. Zhang, Journal of High Energy Physics **2012**, 1 (2012).
- [34] Z. Bern, L. Dixon, D. C. Dunbar, and D. A. Kosower, Nuclear Physics B **425**, 217 (1994), hep-ph/9403226.
- [35] Z. Bern, L. Dixon, D. C. Dunbar, and D. A. Kosower, Nuclear Physics B **435**, 59 (1995).
- [36] Z. Bern, L. J. Dixon, and V. A. Smirnov, Physical Review D **72**, 085001 (2005).
- [37] F. Cachazo, arXiv preprint arXiv:0803.1988 (2008).

- [38] F. Cachazo, M. Spradlin, and A. Volovich, Physical Review D **78**, 105022 (2008).
- [39] R. Britto, F. Cachazo, and B. Feng, Phys. Rev. D **71**, 025012 (2005), hep-th/0410179.
- [40] R. Britto, F. Cachazo, and B. Feng, Nuclear Physics B **715**, 499 (2005), hep-th/0412308.
- [41] R. Britto, F. Cachazo, B. Feng, and E. Witten, Physical Review Letters **94**, 181602 (2005), hep-th/0501052.
- [42] B. Feng and M. Luo, Frontiers of Physics **7**, 533 (2012), arXiv:1111.5759 [hep-th].
- [43] H. Johansson, D. A. Kosower, K. J. Larsen, and M. So-gaard, (2015), arXiv:1503.06711 [hep-th].
- [44] L. Ferro, T. Lukowski, C. Meneghelli, J. Ple-fka, and M. Staudacher, ArXiv e-prints (2013), arXiv:1308.3494 [hep-th].
- [45] S. Franco, D. Galloni, B. Penante, and C. Wen, arXiv preprint arXiv:1502.02034 (2015).
- [46] Z. Bern, J. Carrasco, H. Johansson, and R. Roiban, Phys.Rev.Lett. **109**, 241602 (2012), arXiv:1207.6666 [hep-th].
- [47] I. M. Gelfand, R. M. Goresky, R. D. MacPherson, and V. V. Serganova, Advances in Mathematics **63**, 301 (1987).
- [48] N. E. Mnëv, in *Topology and geometry - Rohlin seminar* (Springer, 1988) pp. 527–543.
- [49] R. Kleiss and H. Kuijf, Nuclear Physics B **312**, 616 (1989).